



# HHS Public Access

Author manuscript

*Nat Chem Biol.* Author manuscript; available in PMC 2009 October 01.

Published in final edited form as:

*Nat Chem Biol.* 2009 April ; 5(4): 244–250. doi:10.1038/nchembio.151.

## HIV-1 and microvesicles from T-cells share a common glycome, arguing for a common origin

Lakshmi Krishnamoorthy<sup>1</sup>, Julian W. Bess Jr.<sup>2</sup>, Alex B. Preston<sup>1</sup>, Kunio Nagashima<sup>3</sup>, and Lara K. Mahal<sup>1,\*</sup>

<sup>1</sup> Department of Chemistry and Biochemistry, Center for Systems and Synthetic Biology and Institute for Cellular and Molecular Biology, University of Texas at Austin, 1 University Station, A5300, Austin, TX 78712-0265.

<sup>2</sup> AIDS Vaccine Program, SAIC-Frederick, Inc., National Cancer Institute at-Frederick, Frederick, MD 21702-1201

<sup>3</sup> Image Analysis Lab, SAIC-Frederick, Inc., National Cancer Institute at-Frederick, Frederick, MD 21702-1201.

### Abstract

HIV-1 is a master at deceiving the immune system, usurping host biosynthetic machinery. Although HIV-1 is coated with host-derived glycoproteins only glycosylation of viral gp120 has been described. Herein we utilize lectin microarray technology to analyze the glycome of intact HIV-1 virions. We show that the glycan coat of human T-cell line-derived HIV-1 matches that of native immunomodulatory microvesicles. The carbohydrate composition of both virus and microvesicles is cell-line dependent, suggesting a mechanism to rapidly camouflage the virus within the host. In addition, binding of both virus and microvesicles to antiviral lectins is enriched over the host cell, raising concern about targeting these glycans for therapeutics. This work also sheds light on the binding of HIV-1 to galectin-1, an important human immune lectin. Overall, our work strongly supports the theory that HIV-1 co-opts the exocytic pathway of microvesicles, potentially explaining why eliciting a protective antiviral immune response is difficult.

---

HIV-1 is a master at deceiving the immune system, making vaccine development a difficult challenge that has yet to be met. At the present time, the ability of HIV-1 to evade an effective immune response is not fully understood 1. HIV-1 takes advantage of host cell machinery to replicate. In T-cells, the virus buds from the cell surface, incorporating a variety of cellular proteins into the viral envelope 2. Whether this process recruits a specific protein subset or the proteins are a random sampling from the cell surface is uncertain, although it is clear that some proteins are enriched or excluded 3-5. Among the enriched proteins are those associated with host-derived particles, designated microvesicles (MV),

---

Users may view, print, copy, and download text and data-mine the content in such documents, for the purposes of academic research, subject always to the full Conditions of use:[http://www.nature.com/authors/editorial\\_policies/license.html#terms](http://www.nature.com/authors/editorial_policies/license.html#terms)

Correspondence should be addressed to L.K.M. (lmalahal@cm.utexas.edu).

Author contributions: L.K. designed and performed research, analyzed data and aided in the writing of the paper. J.W.B. designed and performed research. A.B.P. designed and performed research. K.N. performed research. L.K.M. designed and performed research, analyzed data and wrote the paper.

that are also known to bud from the plasma membrane of T-cells and can contaminate viral preparations 6.

Microvesicles, which include endosomally-derived exosomes, are thought to modulate the immune system. Although their specific functions have yet to be defined, such particles have been found to both stimulate and suppress immune responses 7. The enrichment of a select panel of protein markers (<10) in both microvesicles and HIV-1 has led to the hypothesis that these two particles utilize identical machinery to exit the cell, in essence suggesting that HIV-1 is a pathogenic microvesicle 6, 8-10. In T-cells, it has also been shown that microvesicle protein and lipid markers colocalize to discrete microdomains on the plasma membrane with viral gag and are incorporated into virus-like particles, further strengthening the hypothesis 3. Despite this evidence, whether the two particles share an exit mechanism is still a matter of vigorous debate 11.

The cell surface is coated with carbohydrates on both glycoproteins and glycolipids. These glycans are involved in the sorting of both proteins and lipids to membrane microdomains 12-14. Thus, they may act as molecular markers for trafficking pathways. Carbohydrates are critical to HIV-1 biology, influencing the infectivity of the virus 15. However, the glycosylation of HIV-1 has only been studied with regard to the viral glycoprotein gp120 15, which on average is present in ~20-40 copies per virion 16. The glycosylation of virion-incorporated host proteins, which coat the virus, has largely been ignored and no comparison has been made to the glycome of microvesicles or to the native cell membrane from which both particles arise. A recent advance in glycomic technology, lectin microarrays, has made possible the rapid analysis of the carbohydrate composition of complex biological samples 17-19. Herein, we compare the glycomes of HIV-1, microvesicles and the host membranes of the T-cell lines from which they derive. Our work demonstrates a common glycome for HIV-1 and microvesicles that is cell-line dependent and distinct from the host cell membrane, suggesting that the two particles arise from the same microdomain. We also show that both virus and microvesicles bind strongly to antiviral lectins, emphasizing the need for caution in targeting these glycan epitopes for systemic therapeutic applications. In addition, our arrays reveal a potential new binding motif for galectin-1, an important immune lectin, in the context of HIV-1. Overall, our work presents the first glycomic profile of whole HIV-1 virions and microvesicles, adding crucial evidence to support the pathogenic microvesicle theory of HIV-1.

## RESULTS

### Single color comparison of HIV-1 and MV from H9 cells

For our initial experiments we utilized HIV (HIV-1(MN) CL.4 strain) propagated through the T-cell line H9. HIV-1(MN) CL.4 is a biological clone of HIV-1(MN) that was selected on the basis of high virus yield 20. We compared the glycomic profiles of microvesicles (MV) and cell membrane micellae derived from uninfected H9 cells to HIV using lectin microarrays in a single color format (Fig. 1a and Supplementary Fig. 1a) 17. Previous work has shown that cellular micellae, which originate from isolated cell membranes, contain both glycoproteins and glycolipids and are representative of glycans at the cell surface 17. Our lectin microarrays consisted of ~70 discrete carbohydrate-binding proteins (Supplementary

Table 1). Based on the pattern of fluorescent signals and the known glycan-binding properties of the lectins, the carbohydrate composition of the samples was resolved. For safety reasons we chemically inactivated the HIV with 2,2'-dithiodipyridine (**1**, aldrithiol-2, AT-2) prior to labelling and analysis <sup>21</sup>. This procedure eliminates viral infectivity by covalent modification of free cysteine residues on proteins, but does not affect the structure or function of viral glycoproteins on the virion surface <sup>22</sup>. We observed no differences in the glycomic analysis of AT-2 treated and untreated microvesicle preparations, indicating that, as expected, the inactivation process does not affect the glycome (Supplementary Fig. 1b).

Preliminary examination revealed similar glycopatterns for HIV and MV that varied significantly from that of the host cell membrane (Fig. 1a and Supplementary Fig. 1c, d). Our viral preparation was ~70-80% pure by both electron microscopy and SDS-PAGE analysis (Supplementary Fig. 2a, b), raising concerns that the glycopattern observed might be due to MV contamination. To address this we performed several experiments. First, we tested whether our labelled samples gave signals within the linear range for the majority of lectins at the concentration used in our experiments (~1 µg). Titration experiments confirmed that at the amounts of both HIV and MV used on our arrays, our signals were in the linear signal range (Supplementary Fig. 2c, d). This makes it highly unlikely that similar fluorescence would be observed from the ~5-fold dilution of protein, and thus glycans, which would be expected if our signal was derived only from the contaminating MV component of the HIV sample. In addition, we examined the glycopattern of virus further purified via CD45 immunodepletion. Recent work has shown that T-cell derived microvesicles contain CD45, thus immunodepletion provides highly pure virions virtually devoid of MV <sup>11, 23</sup>. The glycopattern of this highly purified HIV preparation was identical to that observed for the matched undepleted viral sample, confirming that the pattern derives from the virus and not from contaminating MV (Fig. 1b and Supplementary Fig. 2e and Supplementary Methods).

Closer examination of the single color comparison between the uninfected H9 membrane sample, MV from matched uninfected cells and HIV revealed several striking glycomic features that were conserved between HIV and MV from H9 (Fig. 1a and Supplementary Fig. 1d). Both samples were enriched in high mannose epitopes in comparison to the cell membrane as shown by binding to a series of known anti-viral lectins including GNA, NPA, HHL, PSA, ConA, cyanovirin-N (CVN)<sup>24</sup>, scytovirin (SVN)<sup>25</sup> and griffithsin (GRFT)<sup>26, 27</sup>. In addition, MV and HIV were enriched in complex *N*-linked glycans (PHA-L, PHA-E), *N*-acetyllactosamine (LacNAc, lectins: DSA, MAL-I, RCA, STA, WGA), sialic acid (SNA, MAA, MAL-II) and fucosylated (UEA-I, PTL-II, AAL) epitopes. Our lectin microarray data was in concordance with previous studies focused solely on gp120 glycosylation in HIV-1 propagated through the H9 T-cell line which demonstrate the presence of high mannose, LacNAc, complex *N*-linked glycans and sialylation on this glycoprotein <sup>28</sup>. In contrast, blood group antigens A/B (EEA, LBA), which were present on the host cell, were excluded from both HIV and MV. We confirmed the specificity of the lectin interactions via inhibition experiments using a small panel of carbohydrates (Supplementary Fig. 3). Our data suggests that MV and HIV-1 share a conserved exocytic pathway in which particles

incorporate specific cellular glycoproteins as a consequence of budding from discrete domains of the plasma membrane.

### Two-color study of HIV-1 and MV from different T-cells

To extend our initial results, we analyzed uninfected cell membrane micellae, corresponding MVs and HIV virions produced from two other T-cell lines, Jurkat-Tat-CCR5 and SupT1 (Supplementary Figs. 1b and 4 and Supplementary Table 2). To facilitate the direct comparison of these samples to H9-derived samples we utilized a more sensitive ratiometric two-color approach in which the H9 cell membrane micellae were used as a common biological reference (Fig. 2a)<sup>17</sup>. For each of the three cell lines, we analyzed biological replicates consisting of samples from distinct viral (HIV) or cellular (MV) preparations. Both H9 and SupT1 derived virus were the HIV-1(MN) CL.4 strain while Jurkat-Tat-CCR5 derived virus was the parent HIV-1(MN) strain. We observed a conserved metapattern for both MV and HIV regardless of the parent T-cell line (Fig. 2b,  $R=0.66$ ,  $n=48$ ,  $P < 0.0001$ ). As previously discussed for the single color data, this glycopattern was different from that of the parent cell membranes (Fig. 2b,  $R=0.47$ ,  $P < 0.001$  and data not shown) and included increased LacNAc, sialic acid and complex and hybrid *N*-linked glycans on the HIV and MV, and the exclusion of blood group A/B antigen binding from these samples. Surprisingly, HIV clustered more closely with MV from the same parent cell line than with virus propagated through another T-cell line (Fig. 2b, Jurkat-Tat-CCR5,  $R=0.81$ ; H9,  $R=0.86$ ; SupT1,  $R=0.91$ ). This clustering could be accounted for by cell line dependent differences in a select subset of glycans including  $\beta$ -GalNAc (BPA, CSA, VVA), which was higher in Jurkat-Tat-CCR5-derived HIV and MV, and  $\alpha$ -1,2 fucosylated LacNAc (UEA-I, PTA, PTL-II) which was higher in H9-derived HIV and MV. To directly compare the glycomes of our HIV samples, we utilized H9-derived HIV as a reference and hybridized the other HIV samples against it (Fig. 2c). This data confirmed the previously observed glycosylation differences between HIV samples. Our observation that cell line dependent differences in glycosylation were conserved between the MV derived from uninfected cells and the HIV samples reinforces the theory that MV and HIV-1 share a common exocytic pathway.

### Gp120 accounts for glycomic differences of MV and HIV-1

We observed that biological replicates of HIV clustered very tightly (Jurkat-Tat-CCR5,  $R=0.96$ ; H9,  $R=0.98$ , SupT1,  $R=0.97$ ) and were distinguished from MV from the same cell line by increased high mannose levels (ConA, CVN, GNA, GRFT, HHL, NPA, PSA, SVN, UDA, Fig. 2b and Supplementary Fig. 5a). It should be noted that in the T-cell lines studied, high mannose epitopes were enriched in MV compared to the host membranes, thus differences in high mannose between HIV and MV represent a further enrichment in these glycans (Supplementary Fig. 5b). We questioned whether the differences between MV from uninfected cells and HIV could be accounted for simply by the expression of the highly glycosylated viral envelope glycoprotein gp120, which is known for its characteristic high mannose epitopes<sup>29</sup>. To study this, we took advantage of two variants of simian immunodeficiency virus (SIV), SIVmac-NC, which has  $\sim 20$  molecules of gp120 per virion, and the related SIVmac-CP, which has approximately 10-fold higher levels ( $\sim 200$  gp120 molecules per virion)<sup>16, 30</sup>. The SIV was obtained from SupT1 host cells, thus first we

verified that the SIV samples had a similar glycome to both HIV and MV derived from SupT1 ( $R = 0.93$ ,  $n=48$ ,  $P < 0.0001$ , Fig. 3a). Next, using MV from uninfected SupT1 cells as a standard, we directly compared the two SIV variants. We observed higher binding to the gp120 enriched SIVmac-CP than to SIVmac-NC for lectins that commonly discriminated between MV and HIV. A select subset of these lectins is shown in Figure 3b. In general, for lectins that did not differentiate between MV and SIVmac-NC, we did not observe enhanced binding for the SIVmac-CP samples, thus this effect was not attributable to differences in sample labelling (AIA, Fig. 3b). The differences between the SIV variants are most likely a direct consequence of the relative levels of gp120 in the preparations and therefore strongly suggest that the glycomic differences observed between HIV and MV from uninfected cells may be accounted for by the viral envelope glycoprotein gp120.

### Glycans on HIV-1 and MV are enriched in cellular microdomains

Our microarray data indicated that HIV-1 and MV bud from discrete membrane microdomains that can be defined by glycan composition. It has been demonstrated in Jurkat cells that N-Rh-PE (1,2-dipalmitoyl-sn-glycero-3-phosphoethanolamine-*N*-[lissamine rhodamine B sulfonyl], **2**), a fluorescent lipid, labels both microvesicles and membrane microdomains enriched in microvesicle protein markers and HIV-1 gag 3. Therefore we examined whether N-Rh-PE colocalized in microdomains with select fluorescently labelled lectins on the cell surface of our Jurkat-Tat-CCR5 cells. We chose DSA and PHA-L, which bind poly-LacNAc and  $\beta$ -1,6-branched *N*-linked glycans respectively, due to their increased binding to HIV and MV when compared to Jurkat-Tat-CCR5 cell membrane by microarray analysis (Fig. 4a, and Supplementary Fig. 6a). As anticipated, both lectins also showed enrichment in specific microdomains on the plasma membrane that colocalized with N-Rh-PE by fluorescence microscopy (Fig. 4b and Supplementary Fig. 6b). Lectin staining was glycan dependent as demonstrated by abrogation of the signal upon treatment with PNGase F (Fig. 4c and Supplementary Methods). To confirm the plasma membrane as the site of colocalization, we obtained confocal microscopy images from cells labelled with N-Rh-PE and FITC-conjugated DSA (Supplementary Fig. 6c). As previously observed, glycan and lipid markers colocalized at the plasma membrane, again validating our microarray data. Given the high degree of similarity between the glycomes of HIV-1 and microvesicles, our data suggests that the two particles emerge from a specific membrane microdomain that can be defined by glycan epitopes as well as protein and lipid content, pointing to glycosylation as a potential sorting determinant for this domain.

### Bioinformatics implies galectin-1 binds mannose on HIV-1

Galectin-1 is a human immune lectin that binds to LacNAc and has recently been shown to play a role in promoting HIV-1 infectivity in both T cells and macrophages 31, 32. It is thought to aid absorption of the virus to the cells via a bridging interaction mediated by its two identical carbohydrate-binding domains 32. Closer examination of hierarchical clustering of the lectins in our microarray data revealed galectin-1 at the center of a cluster of lectins that bind to high-mannose epitopes (GNA, NPA, HHL, CVN, SVN, GRFT,  $R=0.78$ ,  $n=18$ ,  $P=0.0001$ , Fig. 5a,b), rather than within the cluster of LacNAc binding lectins (LacNAc cluster: MAL-I, RCA, WGA, STA, DSA,  $R=0.87$ ,  $P < 0.0001$ , Fig. 5b). This unexpected result suggested that the binding motif recognized by galectin-1 might be

context dependent and in binding HIV-1, galectin-1 may recognize a high mannose epitope. To further probe whether galectin-1 binds to a high mannose glycan on HIV, we inhibited the H9-derived HIV-galectin-1 interaction on our array with either mannose (3) or the commonly used galectin-1 inhibitor lactose (4). We found mannose to be a better inhibitor of galectin-1 binding to HIV (Fig. 5c) again supporting the idea of interactions via mannose binding. Although we cannot discount the possibility that the immobilization of galectin-1 may have affected the binding of this lectin to glycan epitopes in the context of our arrays, the interactions of microvesicles with galectin-1 could be almost completely inhibited by high concentrations of lactose (Supplementary Fig. 7a and Supplementary Methods), which demonstrated that the galectin-1 on our arrays was active. In contrast, only moderate inhibition by lactose of the HIV-galectin-1 binding was observed. Mannose, however, was an excellent inhibitor of both HIV and MV binding to galectin-1. This suggests that HIV has a stronger interaction with galectin-1 than MV and that this interaction may be based on binding to a mannose epitope. Given that gp120 has highly clustered mannose epitopes, galectin-1 may recognize high mannose in a context dependent manner on HIV in addition to its known LacNAc recognition motif 33.

The idea that galectin-1 recognizes high mannose on HIV-1 has some precedence in the known interactions of galectins-3 and -10 with mannose-containing epitopes 34, 35, although no such reports exist for galectin-1. Additionally mannose-based inhibitors have been reported for both galectin-3 and -9N, indicating molecular mimicry is possible 36. Careful examination of publicly available carbohydrate array data for galectin-1 protein binding from the Consortium for Functional Glycomics glycan array ([www.functionalglycomics.org](http://www.functionalglycomics.org)) also supports our work, revealing binding of galectin-1 to a high mannose epitope at low, but significant, levels (Supplementary Fig. 7b) 33, 37. Taken together, this work suggests that galectin-1 binding to HIV-1 may occur through interactions with the clustered high mannose ligands present on the viral surface in addition to its known interactions with LacNAc residues. Given the role of galectin-1 as an important immune lectin, further investigation into whether high mannose is a context dependent galectin-binding motif, as implied by our data, is warranted.

## DISCUSSION

The components of the host machinery involved in the biogenesis and egress of HIV-1 are yet to be completely unravelled. Several groups have proposed a shared mechanism for microvesicle and HIV-1 exit 8,9, 38. The remarkable similarity of the carbohydrate cloaks of HIV-1 and microvesicles provides the first glycomic evidence for this hypothesis. Glycosylation plays a key role in protein sorting. Our data suggests that the shared glycome of HIV-1 and MV particles from T-cells may reflect a glycan-dependent protein sorting mechanism, which targets host proteins to microdomains from which both microvesicles and HIV particles emerge (Fig. 4). It should be noted, however, that protein trafficking pathways are often cell type dependent and thus HIV-1 in other cell types may utilize alternate mechanisms for exit 39.

Although overall the glycopatterns of microvesicles and viral particles from different T-cell lines display a high similarity, subtle glycomic distinctions exist. As a result of these

differences, HIV-1 has a closer glycome to the microvesicles derived from the same cell line than to the same strain of HIV-1 propagated in a different T-cell line (Fig. 2), again supporting the hypothesis that HIV-1 from T-cells is, in essence, a pathogenic microvesicle. This may allow HIV-1 to rapidly alter its infectivity by passaging through different cells. Indeed, variations in the glycosylation of whole viral particles have been shown to alter the infectivity of the related virus SIV 40.

Immune lectins such as DC-SIGN, a dendritic cell surface protein, and MMR (macrophage mannose receptor) are important portals to cell specific infection for HIV-1 41. In addition, recent work has pointed to a role for galectin-1, a soluble innate immune lectin, in HIV-1 pathogenesis. Galectin-1 is thought to aid infectivity of the virus by providing a bridging interaction between the virus and its host cell surface via homodimeric LacNAc binding 31, 32. Our work calls into question the carbohydrate specificity of the galectin-1-HIV-1 interaction, suggesting that high mannose epitopes may be a significant glycan motif for galectin-1 binding in the context of HIV-1. Our discovery of this phenomenon was a direct consequence of our systems-based approach to glycan analysis. The hierarchical clustering of our lectin data and inhibition with mannose, both experiments that would not have been obvious in a traditional study, revealed this unexpected interaction. Interestingly, galectin-1 has been found on the surface of HIV-1 virions derived from macrophages 42. Given that the protein has no transmembrane domain, this suggests that galectin-1 is tightly associated with glycans on the viral surface. If galectin-1 binds to high mannose epitopes in a context dependent-manner, it would have important implications for the recognition of HIV-1 and other pathogens by this critical immune lectin.

Contrary to our expectation that only HIV-1 would contain significant levels of high mannose epitopes, both microvesicles and HIV-1 were enriched in these glycans (Supplementary Fig. 5). The enrichment of high mannose in both of these particles is a concern, as this epitope is a potential target for both anti-viral lectin based therapies and vaccine development 27, 29. However, significantly higher levels of high mannose were in HIV-1 particles (Fig. 2b). Our data indicates that gp120 is responsible for the differences in glycosylation observed between the microvesicles and HIV-1. This again suggests that HIV-1 has usurped the microvesicle biogenesis pathway in T-cells, hiding from the immune system by wrapping itself in the guise of an immunomodulatory microvesicle. This may contribute to both the dismantling of the immune system by HIV-1 and to the difficulties observed in eliciting a protective immune response to the virus through vaccine strategies 8. Given our lack of knowledge about the role of microvesicles in immune modulation, targeting epitopes, such as high mannose, that functionalize these particles may have unintended negative consequences for the immune system. Our data therefore advocates caution in pursuing this avenue of therapeutic intervention.

## METHODS

### Cell culture

Cell lines H9, SupT1 were obtained from the AIDS Vaccine Program at NCI (Frederick, MD). The Jurkat-Tat-CCR5 cells were obtained from Dr. Quentin Sattentau (University of Oxford, Oxford, England). Cells were cultured in RPMI 1640 (Hyclone, Logan, UT),

supplemented with 2 mM L-glutamine, 10 % fetal bovine serum (Mediatech, Herndon, VA) and penicillin-streptomycin (Invitrogen, Carlsbad, CA) at 37 °C and 5 % CO<sub>2</sub>.

### Cell membrane preparation

We prepared labelled cell membrane micellae from uninfected cells as described previously 17. Briefly, cells were pelleted, washed once in PBS (0.1 M phosphate buffer, 0.15 M NaCl, pH 7.4) and resuspended in ice-cold PBS. Cells were then sonicated on ice (3 × 5 s, 70 % power, Branson sonicator with 1/8" tapered probe tip, Branson, Danbury, CT) to disrupt cell membranes. We then isolated the membranes by pelleting for 1 h at 50,000 rpm using a TLA 100.3 rotor in a Beckman Optima L-80 ultracentrifuge (Beckman Coulter, Fullerton, CA). The pellet was resuspended in Cy buffer (0.1 M Na<sub>2</sub>CO<sub>3</sub>, pH 9.3) and homogenized using a 20 gauge needle ~ 10 ×. The homogenization was repeated using a 27 gauge needle until complete. We determined the protein concentration using the DC protein assay (Bio-Rad, Hercules, CA) and subsequently fluorescently labelled the sample with Cy3- or Cy5-NHS dyes (60 µg of dye per mg of protein, 45 min, RT with gentle rocking, GE Life Sciences, Piscataway, NJ). Excess dye was then removed by dialyzing (6000-8000 Da MW dialysis tubing) into PBS overnight at 4 °C. We again determined the protein concentration for each sample after dialysis prior to hybridization on the microarrays.

### Microvesicles and HIV sample preparation

We collected virus samples from infected cells (*H9*, HIV-1(MN) CL.4 virions; *SupT1*, HIV-1(MN) CL.4, SIVmac-NC and SIVmac-CP virions; *Jurkat-Tat-CCR5*, HIV-1(MN) virions) as previously described 6. We isolated microvesicles from matched uninfected cells. All samples were treated with Aldrithiol-2 21. Samples were resuspended in TNE buffer (0.01 M Tris pH 7.2, 0.1 M NaCl and 1 mM EDTA) and stored at -70 °C prior to labelling.

For fluorescent labelling, pelleted samples (60,000 rpm, 6 min, Beckman TLA-100 centrifuge, TLA100.3 rotor) were resuspended in Cy buffer and then incubated at room temperature for 30 min with Cy3- or Cy5-NHS. Excess free dye was removed from samples by centrifugation through a 20 % sucrose pad (25,000 rpm, 1 h, 4 °C). The pellet was then resuspended in PBS, pelleted (60,000 rpm, 6 min) and diluted in 1 mL of PBS. Labelled samples were stored at -70 °C prior to hybridization to the lectin microarrays.

### Manufacture of Lectin microarrays

The lectin microarrays were manufactured as described previously 17, 18 with minor modifications (see Supplementary Table 1 for lectin list, print concentrations and print monosaccharides). All lectins were purchased from EY Laboratories (San Mateo, CA) with the following exceptions: AAL, HHL, RCA, MAL-I, MAL-II, PTL-I and PTL-II were obtained from Vector Labs (Burlingame, CA), cyanovirin, scytovirin, and griffithsin were gifts from Dr. Barry O'Keefe (NCI-Frederick, Frederick, MD) while galectin-1 43 was a gift from Dr. Linda Baum (UCLA Medical School, Los Angeles, CA).

### Microarray Hybridization

The microarray slides were fitted to the 16-well FAST frame (Schleicher & Schuell, Keene, NH) to create a separate well for each array resulting in a total of 16 sub-arrays per slide.



For single color experiments, we added 1 µg of labelled sample in a final volume of 100 µL (in PBS with 0.05 % Tween) to each sub-array. Samples were hybridized to the lectin microarrays for 2 h at room temperature with gentle rocking. The individual sub-arrays were then rinsed with PBST (PBS, 0.5 % Tween, 5 × 3 min). After a final rinse in PBS, slides were dried prior to scanning. For ratiometric two-color experiments, we used 1 µg of each orthogonally labelled sample in a total volume of 100 µL. Dye-swapped pairs were hybridized for each sample set using the respective Cy3- and Cy5- labelled pairs. We analyzed slides using a GenePix 4000B fluorescent slide scanner (gain = 400, 5 µm scan, Molecular Devices, Sunnyvale, CA) with GenePix Pro 5.1 software. For details on data analysis see Supplementary Methods.

### Fluorescence microscopy

Jurkat cells were labelled with N-Rh-PE (1,2-dipalmitoyl-sn-glycero-3-phosphoethanolamine-*N*-[lissamine rhodamine B sulfonyl], Avanti Polar Lipids, Alabaster, AL) at a final concentration of 5 µM in cold RPMI media. Briefly, we made labelling media by adding the fluorescent lipid to cold media in a glass culture tube using a Hamilton syringe and mixing by vigorous shaking. Prior to labelling, Jurkat cells were washed in cold RPMI media. We then mixed the cells with labelling media and incubated at 4 °C for 1 h. The cells were then washed extensively in cold media and cultured in regular media for an additional 20 h at 37 °C. For fluorescence microscopy, we adhered the cells to poly-lysine coated glass-bottomed dishes for 5 min at 37 °C and incubated with 5 % BSA in modified PBS (mPBS, 3.8 mM KCl, 1.18 mM KH<sub>2</sub>PO<sub>4</sub>, 1.39 mM NaCl, 3.15 mM Na<sub>2</sub>HPO<sub>4</sub>, 1 mM MgSO<sub>4</sub>) for 1 h at room temperature (RT). The cells were then fixed in 3 % paraformaldehyde in mPBS for 15 min, RT. We then washed the cells with mPBS (3 × 5 min) followed by incubation with FITC-labelled DSA (*Datura stramonium* Lectin, EY Labs, 4 µg in 100 µL mPBS + 5 % BSA) or FITC-labelled PHA-L (Phytohemagglutinin-L, EY Labs, 4 µg in 100 µL mPBS + 5% BSA) for 15 min at RT. The cells were subsequently washed with mPBS (3 × 5 min) and images were obtained using an inverted microscope (Nikon Eclipse TE 2000-U; Photometrics CoolSNAP ES monochrome camera) and MetaMorph image analysis software (Version 6.2r6; Molecular Devices) with a 60X oil immersion lens (NA 1.4). FITC and Rhodamine images were obtained using the same dichroic mirror (86012bs, Chroma Technologies, Rockingham Vermont) and separate excitation (ex.) and emission (em.) filters (FITC: ex. S501/16, em S534/30; Rhodamine: ex. S568/24, em. S610/40).

### Supplementary Material

Refer to Web version on PubMed Central for supplementary material.

### ACKNOWLEDGMENTS

We would like to thank; B. Bohn, J. Miller and B. Imming (AIDS Vaccine Program, NCI-Frederick), for help with virus and microvesicle purification, E. Chertova and D. Roser (AIDS Vaccine Program, NCI-Frederick) for biochemical analysis of the samples, D. Graham (U.T. Austin) for generous use of his ultracentrifuge, L. Baum (UCLA Medical School) for the generous gift of galectin-1, B. O'Keefe (NCI-Frederick) for the generous gift of cyanovirin, scytovirin and griffithsin, E. Thoyakulathu for help in the lectin analysis, University of Texas at Austin Microarray Core Facility, and J. Lifson (NCI-Frederick) for insightful reading of the manuscript. In addition, we wish to acknowledge the Consortium for Functional Glycomics (Grant number GM62116) for publicly available

glycan array data from their database used in this work. Funding was provided by the Arnold and Mabel Beckman Foundation (L.K.M.), the National Science Foundation (CAREER CHE-0644530, L.K.M.) and with federal funds from the National Cancer Institute, National Institutes of Health, under contract N01-CO-12400 (J. Bess). The content of this publication does not necessarily reflect the views or policies of the Department of Health and Human Services, nor does mention of trade names, commercial products, or organizations imply endorsement by the U. S. Government.

## REFERENCES

1. Steinbrook R. One step forward, two steps back--will there ever be an AIDS vaccine? *N. Engl. J. Med.* 2007; 357:2653–2655. [PubMed: 18160684]
2. Barre-Sinoussi F, et al. Isolation of a T-lymphotropic retrovirus from a patient at risk for acquired immune deficiency syndrome (AIDS). *Science.* 1983; 220:868–871. [PubMed: 6189183]
3. Booth AM, et al. Exosomes and HIV Gag bud from endosome-like domains of the T cell plasma membrane. *J. Cell Biol.* 2006; 172:923–935. [PubMed: 16533950]
4. Arthur LO, et al. Cellular proteins bound to immunodeficiency viruses: implications for pathogenesis and vaccines. *Science.* 1992; 258:1935–1938. [PubMed: 1470916]
5. Hoxie JA, et al. Nonrandom association of cellular antigens with HTLV-III virions. *Hum. Immunol.* 1987; 18:39–52. [PubMed: 3542913]
6. Bess JW Jr, Gorelick RJ, Bosche WJ, Henderson LE, Arthur LO. Microvesicles are a source of contaminating cellular proteins found in purified HIV-1 preparations. *Virology.* 1997; 230:134–144. [PubMed: 9126269]
7. Keller S, Sanderson MP, Stoeck A, Altevogt P. Exosomes: from biogenesis and secretion to biological function. *Immunol. Lett.* 2006; 107:102–108. [PubMed: 17067686]
8. Gould SJ, Booth AM, Hildreth JE. The Trojan exosome hypothesis. *Proc. Natl. Acad. Sci. U. S. A.* 2003; 100:10592–10597. [PubMed: 12947040]
9. Gluschankof P, Mondor I, Gelderblom HR, Sattentau QJ. Cell membrane vesicles are a major contaminant of gradient-enriched human immunodeficiency virus type-1 preparations. *Virology.* 1997; 230:125–133. [PubMed: 9126268]
10. Nguyen DG, Booth A, Gould SJ, Hildreth JE. Evidence that HIV budding in primary macrophages occurs through the exosome release pathway. *J. Biol. Chem.* 2003; 278:52347–52354. [PubMed: 14561735]
11. Coren LV, Shatzer T, Ott DE. CD45 immunoaffinity depletion of vesicles from Jurkat T cells demonstrates that exosomes contain CD45: no evidence for a distinct exosome/HIV-1 budding pathway. *Retrovirology.* 2008; 5:64. [PubMed: 18631400]
12. Hakomori S. Carbohydrate-to-carbohydrate interaction, through glycosynapse, as a basis of cell recognition and membrane organization. *Glycoconj. J.* 2004; 21:125–137. [PubMed: 15483378]
13. Brewer CF, Miceli MC, Baum LG. Clusters, bundles, arrays and lattices: novel mechanisms for lectin-saccharide-mediated cellular interactions. *Curr. Opin. Struct. Biol.* 2002; 12:616–623. [PubMed: 12464313]
14. Huet G, et al. Involvement of glycosylation in the intracellular trafficking of glycoproteins in polarized epithelial cells. *Biochimie.* 2003; 85:323–330. [PubMed: 12770771]
15. Balzarini J. Targeting the glycans of gp120: a novel approach aimed at the Achilles heel of HIV. *Lancet Infect. Dis.* 2005; 5:726–731. [PubMed: 16253890]
16. Chertova E, et al. Envelope glycoprotein incorporation, not shedding of surface envelope glycoprotein (gp120/SU), is the primary determinant of SU content of purified human immunodeficiency virus type 1 and simian immunodeficiency virus. *J. Virol.* 2002; 76:5315–5325. [PubMed: 11991960]
17. Pilobello KT, Slawek DE, Mahal LK. A ratiometric lectin microarray approach to analysis of the dynamic mammalian glycome. *Proc. Natl. Acad. Sci. U. S. A.* 2007; 104:11534–11539. [PubMed: 17606908]
18. Hsu KL, Mahal LK. A lectin microarray approach for the rapid analysis of bacterial glycans. *Nat. Protoc.* 2006; 1:543–549. [PubMed: 17406280]
19. Kuno A, et al. Evanescent-field fluorescence-assisted lectin microarray: a new strategy for glycan profiling. *Nat. Methods.* 2005; 2:851–856. [PubMed: 16278656]

20. Ott DE, Nigida SM Jr, Henderson LE, Arthur LO. The majority of cells are superinfected in a cloned cell line that produces high levels of human immunodeficiency virus type 1 strain MN. *J. Virol.* 1995; 69:2443–2450. [PubMed: 7884892]
21. Rossio JL, et al. Inactivation of human immunodeficiency virus type 1 infectivity with preservation of conformational and functional integrity of virion surface proteins. *J. Virol.* 1998; 72:7992–8001. [PubMed: 9733838]
22. Chertova E, et al. Sites, mechanism of action and lack of reversibility of primate lentivirus inactivation by preferential covalent modification of virion internal proteins. *Curr. Mol. Med.* 2003; 3:265–272. [PubMed: 12699362]
23. Trubey CM, et al. Quantitation of HLA class II protein incorporated into human immunodeficiency virus type 1 virions purified by anti-CD45 immunoaffinity depletion of microvesicles. *J. Virol.* 2003; 77:12699–12709. [PubMed: 14610192]
24. Bolmstedt AJ, O'Keefe BR, Shenoy SR, McMahon JB, Boyd MR. Cyanovirin-N defines a new class of antiviral agent targeting N-linked, high-mannose glycans in an oligosaccharide-specific manner. *Mol. Pharmacol.* 2001; 59:949–954. [PubMed: 11306674]
25. Bokesch HR, et al. A potent novel anti-HIV protein from the cultured cyanobacterium *Scytonema varium*. *Biochemistry.* 2003; 42:2578–2584. [PubMed: 12614152]
26. Mori T, et al. Isolation and characterization of griffithsin, a novel HIV-inactivating protein, from the red alga *Griffithsia* sp. *J. Biol. Chem.* 2005; 280:9345–9353. [PubMed: 15613479]
27. Balzarini J. Inhibition of HIV entry by carbohydrate-binding proteins. *Antiviral. Res.* 2006; 71:237–47. [PubMed: 16569440]
28. Mizuochi T, et al. Diversity of oligosaccharide structures on the envelope glycoprotein gp 120 of human immunodeficiency virus 1 from the lymphoblastoid cell line H9. Presence of complex-type oligosaccharides with bisecting *N*-acetylglucosamine residues. *J. Biol. Chem.* 1990; 265:8519–8524. [PubMed: 2341393]
29. Scanlan CN, Offer J, Zitzmann N, Dwek RA. Exploiting the defensive sugars of HIV-1 for drug and vaccine design. *Nature.* 2007; 446:1038–1045. [PubMed: 17460665]
30. LaBranche CC, et al. Biological, molecular, and structural analysis of a cytopathic variant from a molecularly cloned simian immunodeficiency virus. *J. Virol.* 1994; 68:5509–5522. [PubMed: 8057433]
31. Mercier S, et al. Galectin-1 promotes HIV-1 infectivity in macrophages through stabilization of viral adsorption. *Virology.* 2008; 371:121–129. [PubMed: 18028978]
32. Ouellet M, et al. Galectin-1 acts as a soluble host factor that promotes HIV-1 infectivity through stabilization of virus attachment to host cells. *J. Immunol.* 2005; 174:4120–4126. [PubMed: 15778371]
33. Stowell SR, et al. Galectins-1, -2 and -3 exhibit differential recognition of sialylated glycans and blood group antigens. *J. Biol. Chem.* 2008; 283:10109–10123. [PubMed: 18216021]
34. Kohatsu L, Hsu DK, Jegalian AG, Liu FT, Baum LG. Galectin-3 induces death of *Candida* species expressing specific beta-1,2-linked mannans. *J. Immunol.* 2006; 177:4718–4726. [PubMed: 16982911]
35. Swaminathan GJ, Leonidas DD, Savage MP, Ackerman SJ, Acharya KR. Selective recognition of mannose by the human eosinophil Charcot-Leyden crystal protein (galectin-10): a crystallographic study at 1.8 Å resolution. *Biochemistry.* 1999; 38:13837–13843. [PubMed: 10529229]
36. Tejler J, Skogman F, Leffler H, Nilsson UJ. Synthesis of galactose-mimicking 1H-(1,2,3-triazol-1-yl)-mannosides as selective galectin-3 and 9N inhibitors. *Carbohydr. Res.* 2007; 342:1869–1875. [PubMed: 17407769]
37. Blixt O, et al. Printed covalent glycan array for ligand profiling of diverse glycan binding proteins. *Proc. Natl. Acad. Sci. U. S. A.* 2004; 101:17033–17038. [PubMed: 15563589]
38. Esser MT, et al. Differential incorporation of CD45, CD80 (B7-1), CD86 (B7-2), and major histocompatibility complex class I and II molecules into human immunodeficiency virus type 1 virions and microvesicles: implications for viral pathogenesis and immune regulation. *J. Virol.* 2001; 75:6173–6182. [PubMed: 11390619]

39. Ono A, Freed EO. Cell-type-dependent targeting of human immunodeficiency virus type 1 assembly to the plasma membrane and the multivesicular body. *J. Virol.* 2004; 78:1552–1563. [PubMed: 14722309]
40. Gaskill PJ, Zandonatti M, Gilmartin T, Head SR, Fox HS. Macrophage-derived simian immunodeficiency virus exhibits enhanced infectivity by comparison with T-cell-derived virus. *J. Virol.* 2008; 82:1615–1621. [PubMed: 18045942]
41. Vigerust DJ, Shepherd VL. Virus glycosylation: role in virulence and immune interactions. *Trends Microbiol.* 2007; 15:211–218. [PubMed: 17398101]
42. Chertova E, et al. Proteomic and biochemical analysis of purified human immunodeficiency virus type 1 produced from infected monocyte-derived macrophages. *J. Virol.* 2006; 80:9039–9052. [PubMed: 16940516]
43. Pace KE, Hahn HP, Baum LG. Preparation of recombinant human galectin-1 and use in T-cell death assays. *Methods Enzymol.* 2003; 363:499–518. [PubMed: 14579599]

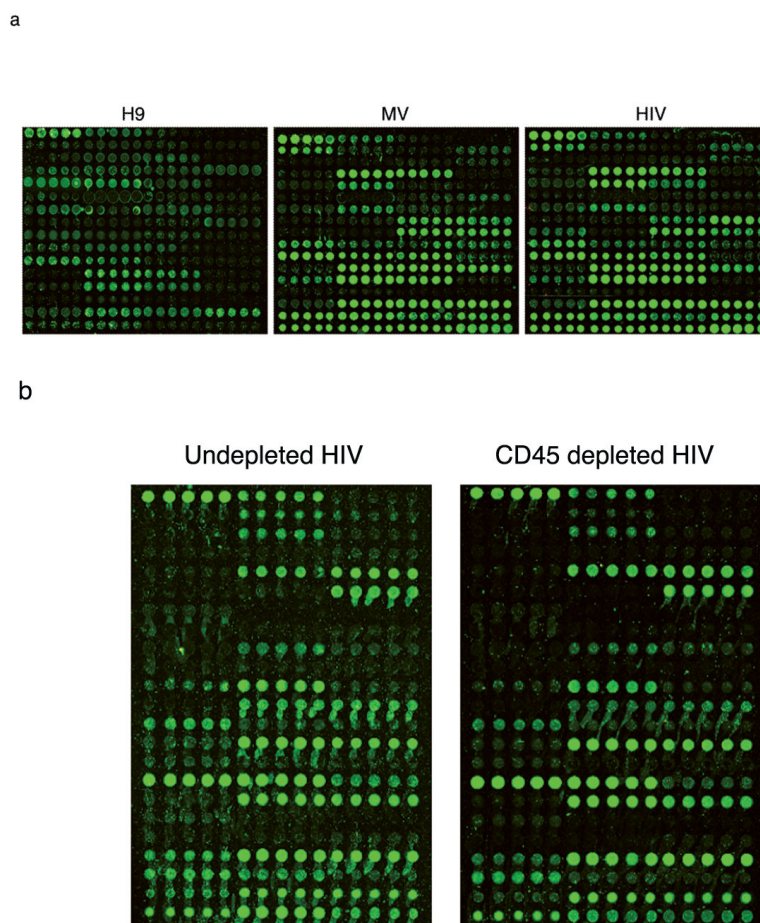
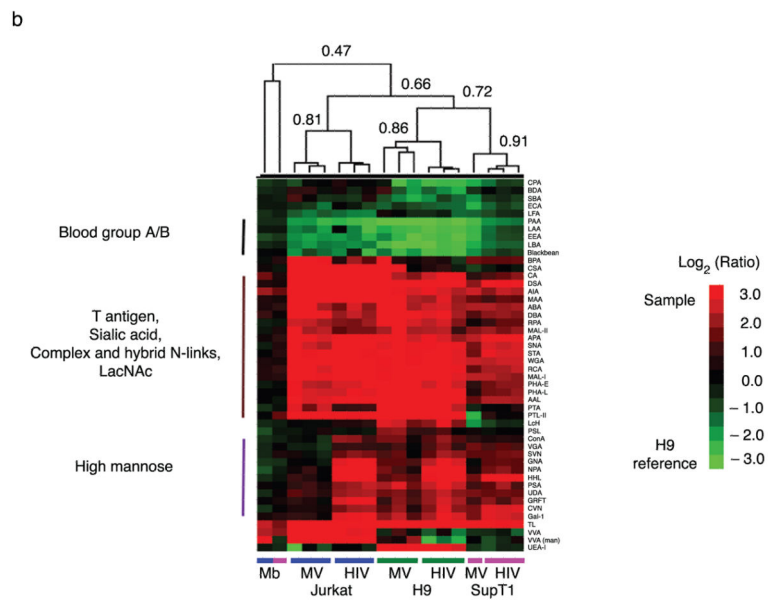
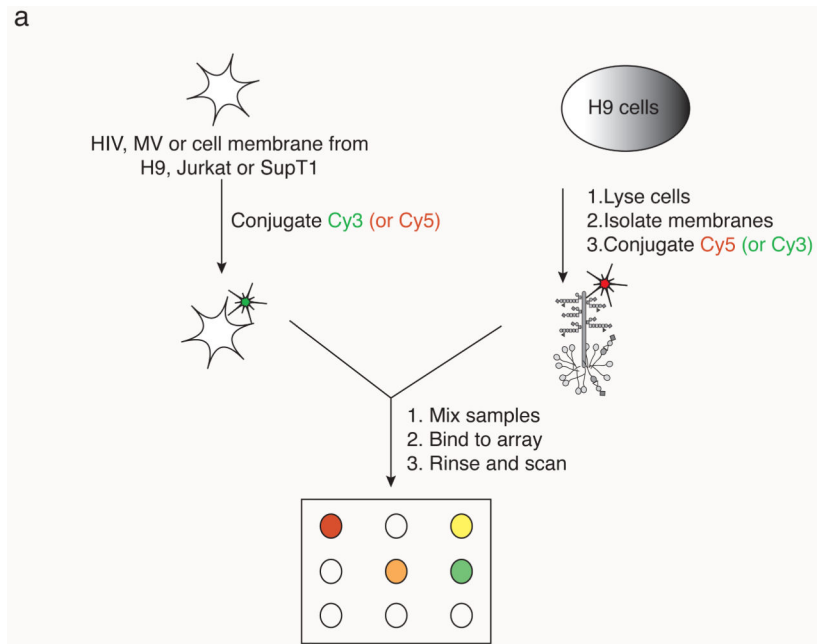


**Figure 1. Glycomic profiling of HIV and uninfected cell membrane and microvesicles derived from H9 cells**

(a) Equal amounts of Cy3-labelled sample (1  $\mu$ g, based on protein concentration) were hybridized to the arrays. Cell membrane micellae and MV were derived from uninfected H9 cells. HIV samples were obtained from HIV-1(MN) CL.4 strain infected H9 cells. Data shown is representative of 3 independent experiments. (b) Cy3-labelled ultra-purified CD45 immunodepleted virus was compared to equivalent amounts (based on p24 levels) of matched undepleted HIV via lectin microarray analysis.



c

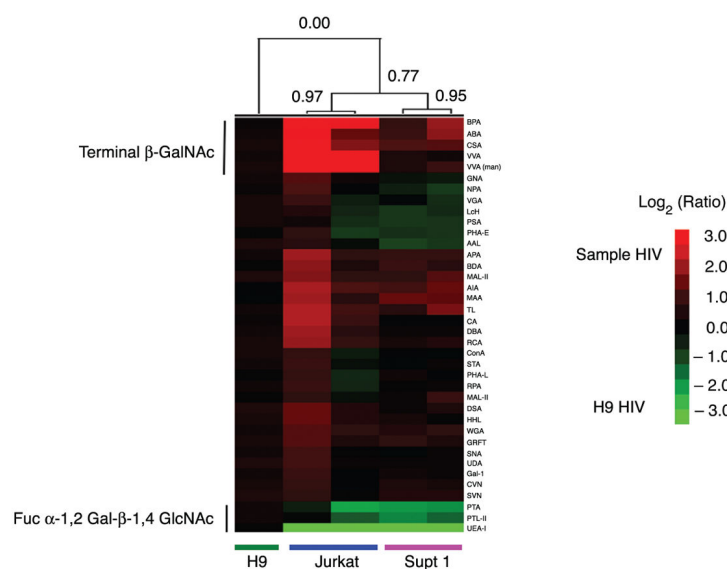


**Figure 2. Ratiometric comparison of HIV-1 to uninfected cell membrane and microvesicles from three T-cell lines**

(a) Experimental scheme. (b) H9 membrane was the common biological reference for comparison of MV and HIV derived from different T-cell lines (H9 (green line), Jurkat-Tat-CCR5 (Jurkat, blue line), and SupT1 (pink line)) and their respective cell membranes (Mb, n=1). Biological replicates from distinct viral (HIV; n=3 for each cell line) or microvesicle (MV; n=3 for H9 and Jurkat, n=1 for SupT1) preparations were analyzed. A dye-swapped pair of arrays was analyzed for each sample. Only lectins positive on at least one array were considered in our analysis. Yang correlation values were obtained for the data set and used to generate hierarchically clustered heat maps with the Pearson correlation coefficient as the distance metric (n=48), and average linkage analysis 17. Coefficients are shown for each major branch. To facilitate visualization, lectins were clustered using the Euclidean distance metric (y-axis). Red indicates enhanced binding to the sample while green indicates enhanced binding to H9 membrane. Data shown is representative of 3 replicate experiments. (c) Direct comparison of HIV glycosylation. H9-, Jurkat- and SupT1-derived HIV (n=2) were hybridized against H9-derived HIV (biological reference). A dye-swapped pair of arrays was run for each sample to generate Yang correlations as before. The heat map with Pearson correlation coefficients is shown. Red indicates enhanced binding to the varying HIV samples while green indicates enhanced binding to the H9-derived HIV. Data is representative of 3 replicate experiments.

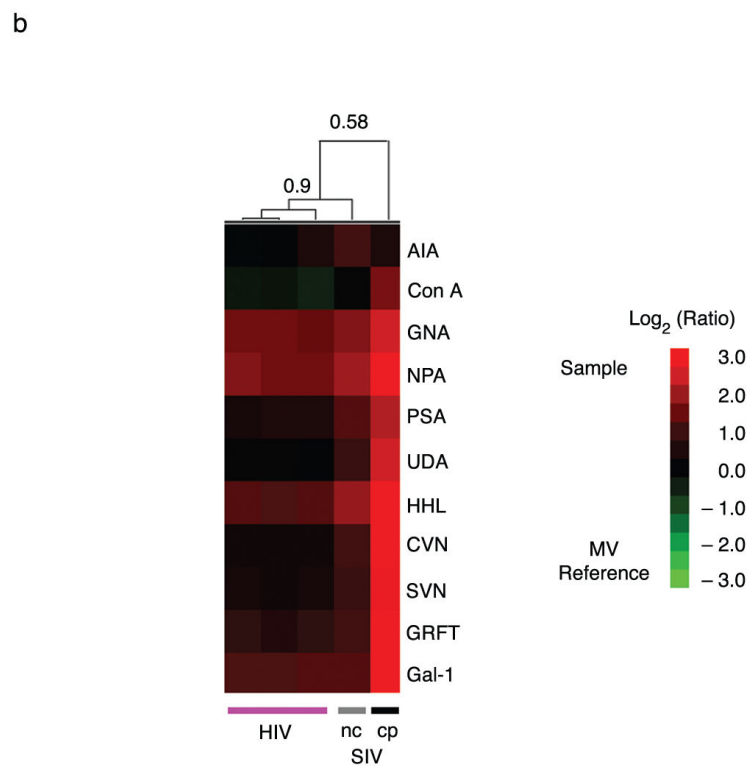
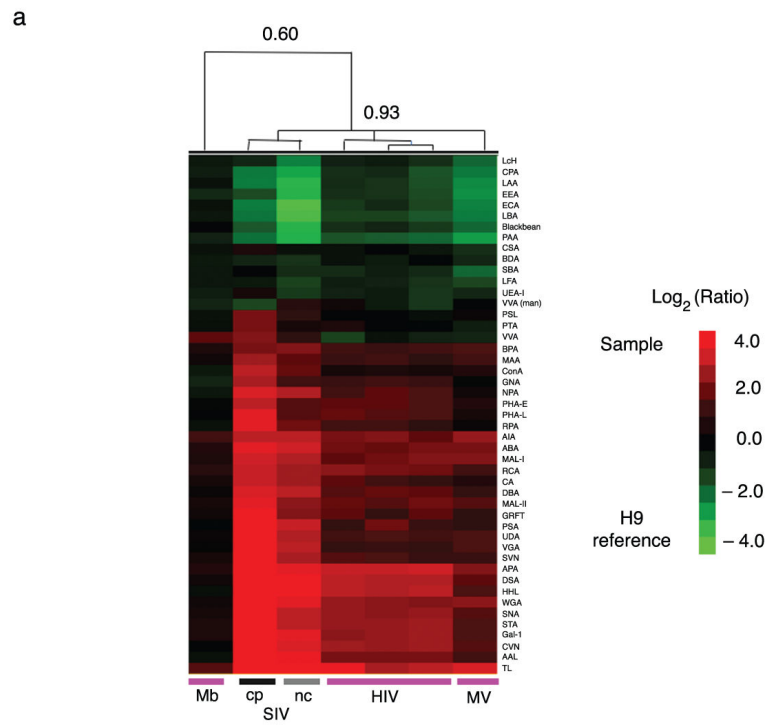


**Figure 3. Gp120 glycosylation may account for the differences observed between MV and HIV**  
**(a)** SupT1-derived SIV share glycomic markers with HIV and MV derived from SupT1. Briefly, labelled HIV (n=3 biological replicates), SIVmac-NC (n=1, nc, grey line), SIVmac-



CP (n=1, cp, black line), MV (n=1) and SupT1 membrane (n=1, Mb) samples were hybridized against H9 membrane (biological reference) as before. The hierarchical cluster map with Pearson correlation coefficients at select branches is shown. Red indicates enhanced binding to the sample while green indicates enhanced binding to the reference (H9 membrane). Data is representative of 3 replicate experiments. **(b)** Direct comparison of the glycomes of SIVmac-NC, SIVmac-CP and HIV. Equal amounts of the SupT1-derived HIV and SIV samples from **(a)** were hybridized against MV derived from uninfected SupT1 cells (biological reference), with two arrays (dye-swapped pair) run for each sample to generate Yang correlations as before. The hierarchical cluster map of a select group of lectins with Pearson correlation coefficients is shown. Red indicates enhanced binding to the sample while green indicates enhanced binding to the SupT1-derived MV reference. Data shown are representative of 3 replicate experiments.

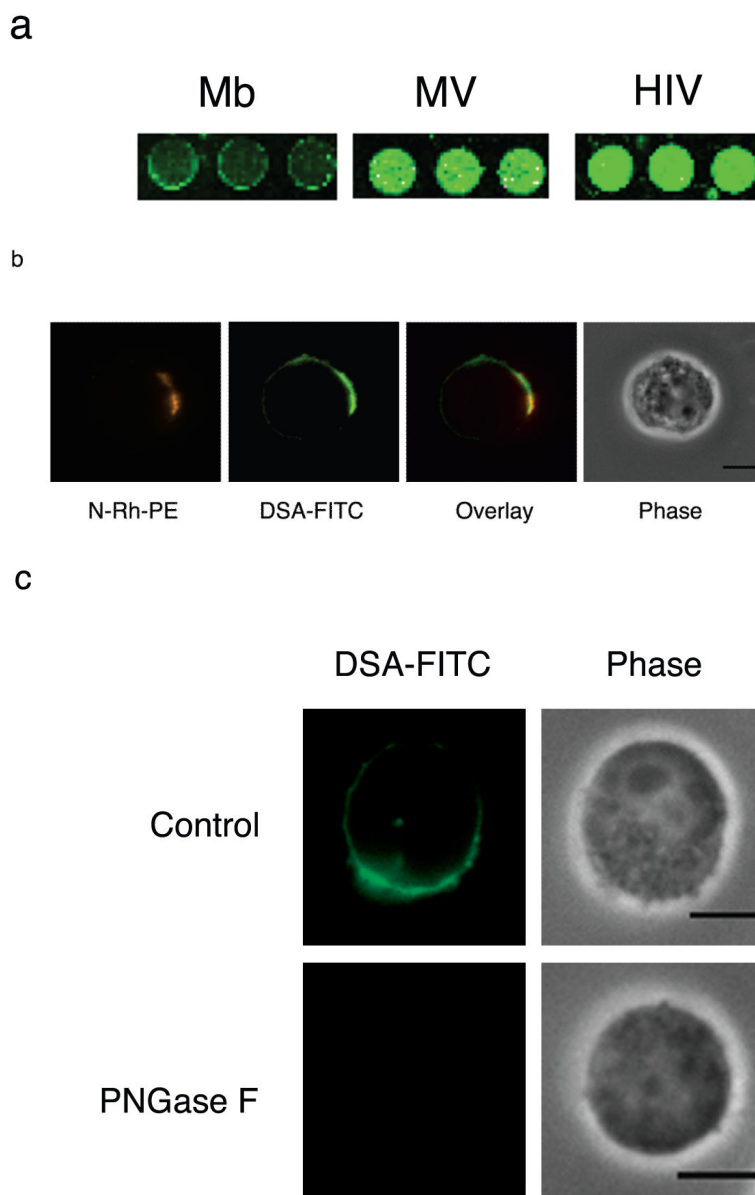


**Figure 4. N-Rh-PE enriched domains co-localize with FITC-labeled lectins on Jurkat-Tat-CCR5 (Jurkat) cell surfaces**

(a) MV and HIV-1 from Jurkat cells exhibit increased binding to DSA in comparison to the Jurkat cell membrane (Mb). Data shown is representative of 3 independent experiments. (b) Jurkat cells were labelled with N-Rh-PE at 4 °C for 1 hr, followed by 20 h of growth in normal media at 37 °C. Cells were then fixed, stained with FITC-conjugate DSA and examined using fluorescence microscopy. N-Rh-PE domains (red) colocalized with domains that were enriched in glycans recognized by DSA (green). Data shown is representative of cells observed in 3 independent experiments. (c) Jurkat cells fixed for microscopy were treated with PNGase F to remove *N*-linked glycans prior to staining with DSA-FITC. As expected, a loss of DSA-FITC staining was observed, confirming that the lectin is interacting with cell surface carbohydrates. Shown are representative images of the DSA-

FITC stained PNGase F-treated cells (PNGase F) and an untreated control (Control) from a minimum of 5 fields of view (~10-15 cells per field) per treatment. Images were taken under identical microscopy conditions and are set to the same scale.

Author Manuscript

Author Manuscript

Author Manuscript

Author Manuscript

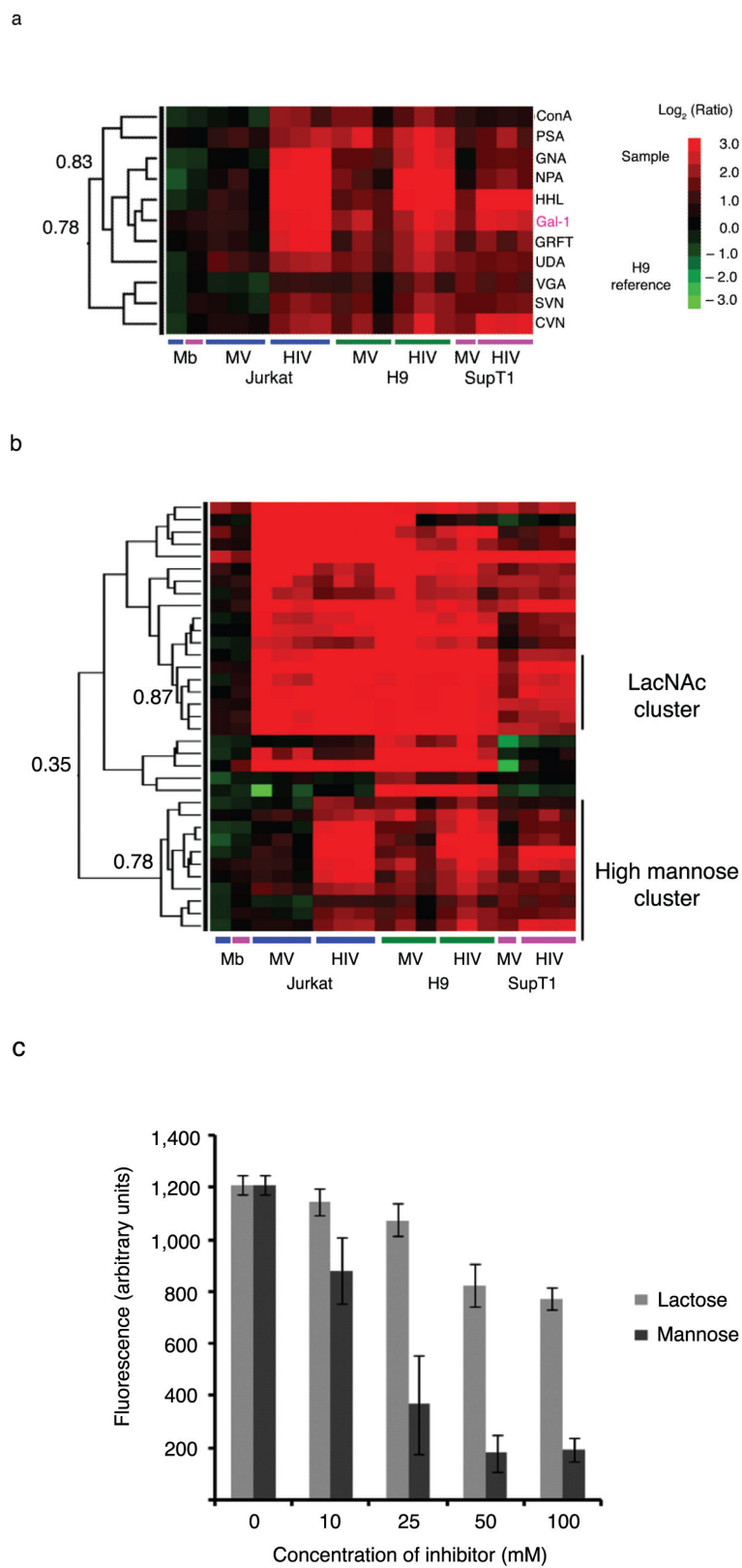


**Figure 5. Evidence that galectin-1 is a high mannose binder**

(a) Galectin-1 (Gal-1, pink) clustered tightly with mannose binding lectins ( $R = 0.83$ ,  $n=18$ ,  $P < 0.0001$ ). Data used for the hierarchical clustering was identical to that in Figure 2b. Lectins were clustered using the Pearson correlation coefficient as the distance metric and average linkage analysis. A portion of the heat map is displayed with the Pearson correlation coefficients indicated for selected branch points. (b) Galectin-1 did not cluster with other LacNAc binding lectins ( $R = 0.36$ ,  $n=18$   $P = 0.142$ ). (c) Mannose is a better inhibitor than lactose for galectin-1-HIV interactions. Lectin microarrays containing galectin-1 (1 mg/mL print concentration) were preincubated with varying concentrations of either lactose or mannose, followed by addition of Cy3-labelled H9-derived HIV samples. The graph represents the average background-subtracted median fluorescence (arbitrary units) of 4 spots from arrays treated with varying concentrations of sugar (lactose, light grey; mannose, dark grey). The final concentration of the carbohydrate inhibitor is shown. Error bars represent the standard deviation for the 4 spots. Data shown is representative of 2 independent experiments.